MATERIALS PHYSICS AND MECHANICS RESEARCH ARTICLE

Submitted: November 5, 2025 **Revised: December 3, 2025** **Accepted: December 6, 2025**

Influence of the core-sleeve boundary interface on the composite Al-Al wire properties

A.E. Medvedev [1]✉, A.F. Shaikhulova [1], M.M. Motkov [2], M.Yu. Murashkin [1]

[1] Ufa University of Science and Technology, Ufa, Russia

[2] Siberian Federal University, Krasnoyarsk, Russia

✉ medvedevandreyrf@gmail.com

ABSTRACT

The influence of the core-sleeve boundary interface on the mechanical properties and electrical conductivity of the composite all-aluminium wires made of electromagnetically cast Al-0.5 wt. % Fe and Al-1.7 wt. % Fe alloys was studied. For the comparison all-aluminium wires made of same materials were studied as well. Structural analysis was presented by the scanning electron microscopy of the composite all-aluminium wires cross-section, as well as by the fractographic analysis of the failed tensile samples. It was demonstrated that the effect of the core-sleeve boundary increases with the increase in amount of alloying elements in the composite all-aluminium wires components. The core-sleeve boundary in the composite all-aluminium wires acts as a buffer for the deformation thus the amount of the deformation, that otherwise would be distributed gradually in the all-aluminium wires, is distributed uneven between the core and the sleeve of the composite all-aluminium wires, accumulating more within the composite all-aluminium wires sleeve. The major influence of the core-sleeve boundary is noted in yield strength and ductility of the wires, while electrical conductivity and especially ultimate tensile strength remain mostly unaffected.

KEYWORDS

aluminium alloys • electromagnetic crystallization • composite wire • mechanical strength • ductility electrical conductivity

Funding. *The research was supported by the Russian Science Foundation grant No. 25-19-00633, https://rscf.ru/project/25-19-00633/.*

Acknowledgements. *The authors express special gratitude to the Center for Collective Use "Nanotech" of the Federal State Budgetary Educational Institution of Higher Education "Ufa University of Science and Technology".*

Citation: Medvedev AE, Shaikhulova AF, Motkov MM, Murashkin MYu. Influence of the core-sleeve boundary interface on the composite Al-Al wire properties. *Materials Physics and Mechanics*. 2025;53(6): 190–200. http://dx.doi.org/10.18149/MPM.5362025_14

Introduction

Aluminum and its alloys may replace copper as electrically conductive materials because they are lightweight, commercially available, exhibit high electrical conductivity, and are resistant to corrosion [1]. The downside of the aluminium alloys is their relatively low strength, making it important to find either new alloys or methods of their production. One result of the search for new conductive materials has been the concept of creating hybrid (composite) materials [2,3]. This way two or more different materials could be united into one product, theoretically combining all the advantages of each individual component without their disadvantages [4,5].

This approach, for example, has been implemented in the form of a specific cable architecture consisting of a core and an outer layer made of various aluminum alloys, such as an all-aluminum alloy cable (AAAC) [6] and an aluminum cable steel-reinforced

(ACSR) [7]. In these cases, hybridization of the final product is achieved through the mechanical assembly of different materials. The most obvious approach to the hybridization of aluminum alloys is the creation of composite materials from various aluminum alloys [8,9]. Combining them in a certain proportion can help overcome the tradeoff between strength and conductivity, providing both high mechanical strength and high electrical conductivity in a composite aluminum alloy [10]. Previous studies have shown the potential of this approach to produce Al-Al composite wire [11].

The other way to create composite aluminium alloys is the application of cold bonding, for example, the accumulative roll bonding (ARB) [12–14]. Such approaches make it possible to obtain gradient microstructures that provide effective control over a complex of structurally sensitive characteristics. The main advantages of this approach are the possibility to produce continuous products and the high deformation value required for the mechanical bonding of materials [15]. Unfortunately, ARB is not suitable for wire production.

Research into the production of composite conductors made from two alloys using the "core-sleeve" design has shown that the drawing process used to produce them has not yet resulted in a monolithic blank [16]. This is apparently due to the fact that a single drawing pass of such composite blanks can only achieve a deformation of 30 %, whereas reliable joining of different metals/alloys to create a composite sample using ARB requires a deformation of at least 50 % at elevated temperatures (0.3–0.4 of a melting temperature) [17].

Therefore, composite conductors made from aluminum alloys currently contain an interface between their components. In this regard, it is important to determine how the presence and the length of the interface between components influences the properties of such conductors.

In this study, the composite aluminium wires made of Al-0.5 wt. % Fe and Al-1.7 wt. %Fe were compared to the all-aluminium wires made of same materials. The length of the core-sleeve boundary interface was chosen so that the fraction of the core would be 10 % in the cross-section. The choice of the materials was based on the fact that these alloys belong to immiscible systems and that the absence of the solid solution effect and the associated diffusion processes will allow to isolate the influence of the boundary interface, without taking into consideration potential diffusion transitions of alloying elements through it.

Materials and Methods

Two alloys of the Al-Fe system with an iron content of 0.5 and 1.7 wt. % were used as research material. Initial samples were produced in the form of rods of a diameter of 11 mm by continuous casting in an electromagnetic mold (EMC) [18]. The chemical composition of the alloy samples is presented in Table 1.

Table 1. Chemical composition of alloys of the Al-Fe system (wt. %)

Alloy	Fe	Si	Cu	Mg	Zn	∑Ti,Mn,Cr	Al
Al-0.5Fe	0.50	0.04	0.01	0.01	0.02	⩽ 0.02	Rem.
Al-1.7Fe	1.65	0.03	0.01	-	0.03		

Samples of 11 mm in diameter wire rod of the Al-Fe alloys were made on the basis of primary aluminum grade A85 (not less than 99.85 wt. % Al) and Fe80Al20 alloys in proportions selected to match the required Fe concentrations. After the melt temperature reached more than 800 °C, continuous casting was carried out in an EMC installation at a speed of 12.4 mm/s.

Part of the Al-0.5Fe and Al-1.7Fe alloys samples were cold drawn (CD) down to 3 mm diameter, creating all-aluminium wires (Al-0.5Fe AAW and Al-1.7Fe AAW). The other part of the Al-1.7Fe and Al-0.5Fe alloys rods were cold drawn down to 10 mm diameter. The section of these rods with 300 mm in length was cut off. Then the hole of 3.2 mm in diameter was drilled along the longitudinal axis of the cut samples, creating the tubes. The inner surface of the tubes and the outer surface of the wires of both samples were cleaned and degreased, after which the wire was put into the corresponding tube. The combined billet was subjected to CD with an area reduction of 91 %. Total area reduction was achieved in 10 passes, resulting in the 3 mm diameter composite all-aluminium wires of the following compositions: Al-0.5Fe core and Al-0.5Fe sleeve; Al-1.7Fe core and Al-1.7Fe sleeve (Al-0.5Fe CAAW and Al-1.7Fe CAAW, respectively). Thus, the fraction of the core in the cross-section of CAAW was 10 %, and the length of the core-sleeve boundary interface was 30 % of the outer wire diameter. The evaluation of the core fraction in the cross-section of the wire using scanning electron microscopy (SEM) images. This cross-section corresponds to the length of the interface being the 30 % of the outer wire diameter.

The heat resistance of wire samples was assessed in accordance with the requirements of the IEC 62641:2023 standard [19]. To do this, after CD, samples were annealed at a temperature of 230 °C for 1 h, followed by cooling in air. The microstructure was studied using scanning electron microscopy (SEM) on a Tescan Mira microscope at an accelerating voltage of 10–20 kV in back-scattered (BSE) and secondary electrons (SE) modes. To obtain statistically reliable results, tensile tests were carried out on three samples for each state, on a universal tensile machine Instron 5982 at room temperature and at a speed of 100 mm/min. Based on the test results, the values of the yield strength ($\sigma_{0.2}$), ultimate tensile strength (σ_{UTS}) and elongation to failure (δ) were determined [20].

The specific electrical resistance of the material under study was measured in accordance with IEC 60468:1974 [21]. Straightened samples of at least 1 m in length were selected. The electrical conductivity value of the samples relative to annealed copper (International Annealed Copper Standard) was calculated using the equation:

$$IACS = \rho_{Cu}/\rho_{Al} \times 100\ [\%], \quad (1)$$

where ρ_{Al} is the experimentally determined value of the specific electrical resistance of the aluminum alloy sample, ρ_{Cu} is the specific electrical resistance of annealed copper, equal to 17.241 nΩm.

Results and Discussion

The cross-section of the Al-0.5Fe CAAW and Al-1.7Fe CAAW is presented on Fig. 1. The initial placement of the core wire was designed to be coaxial, the displacement of the core wire from the center of the sleeve is probably due to the bending of the drill instrument during preparation of the tube (see Materials and Methods section). Gaps in

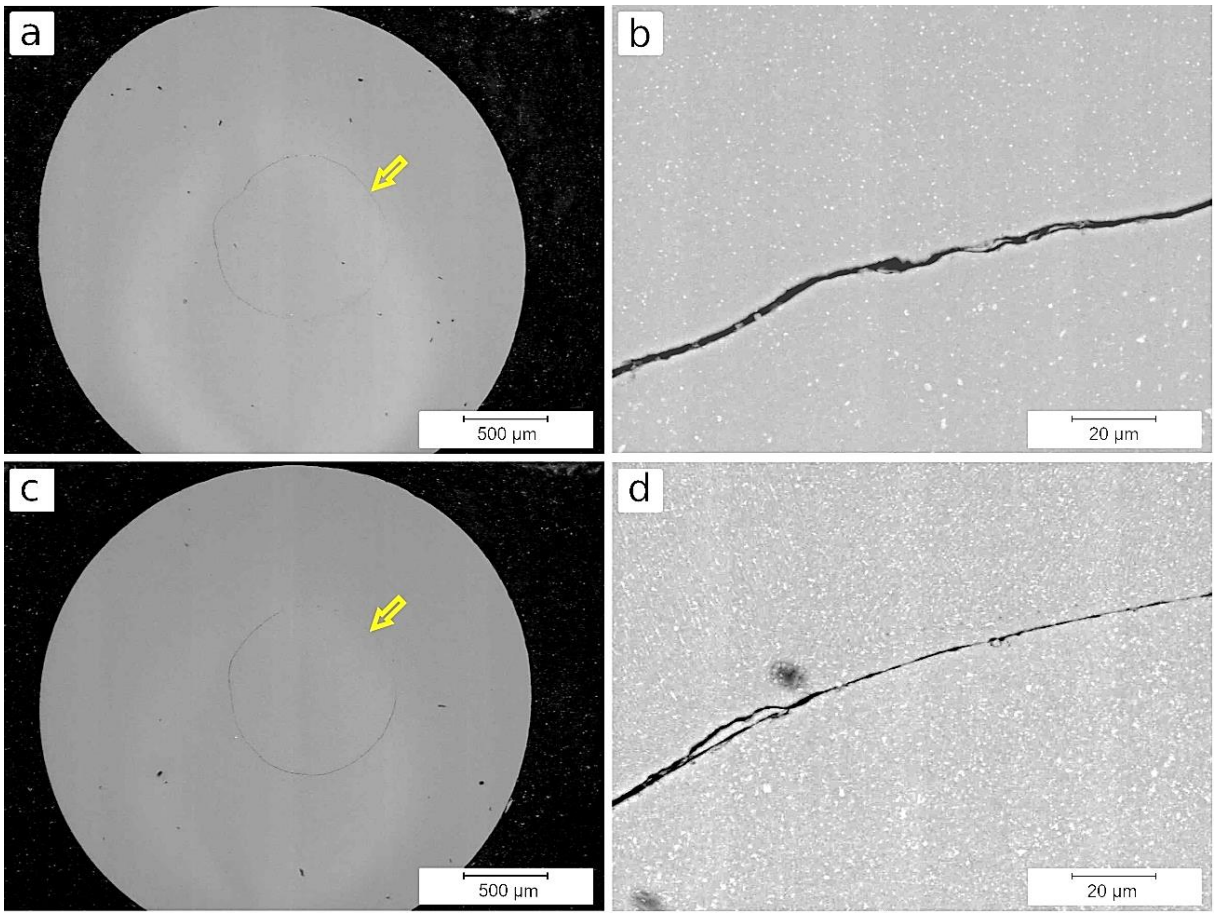

Fig. 1. Cross-section of the Al-0.5Fe CAAW (a,b) and Al-1.7Fe CAAW (c,d), SEM BSE. Yellow arrows point at the core of the CAAW

core-sleeve boundary interface are the consequence of the drilling a hole in the initial billet, and surface quality depends on the drillling method and tool. Still, for the better CAAW performance improving the contact surface quality may be recommended. Nevertheless, this doesn't affect the performance of the CAAWs, since the fraction of the core in both alloys is 10 ± 1 %. Cross-section of the wires shows deviation from the circular shape, although it also doesn't affect the overall CAAW performance.

Al-1.7Fe CAAW (Fig. 1(c,d)) demonstrates notably higher, compared to Al-0.5Fe CAAW (Fig. 1(a,b)), fraction of the second phase particles, being of the Al_xFe_y nature, most probably Al_2Fe or Al_6Fe [22,23]. Figure 1 also demonstrates the core-sleeve boundary of the CAAWs. The applied pressure and temperature were clearly not enough to form a continuous bond between materials, leaving the gap from 30 to 300 nm in width (Fig. 1(b,d)). In works related to ARB it is stated that the deformation value at each pass should be at least 50 % in order to mechanically bond the contact materials, while in this case it was notably lower [12]. It would be promising to increase the deformation value of each drawing pass or even include the extrusion stage in order to close the gap on the core-sleeve boundary. Based on the previous study it is safe to say that annealing at 230 °C didn't affect the core-sleeve boundary [24].

Table 2 contains the data of the mechanical and physical properties of the composite all-aluminium wires (CAAWs), as well as data for the all-aluminium wires (AAWs).

Table 2. Physical and mechanical properties of the CAAW

Sample	Electrical conductivity		σ_{YS}		σ_{UTS}		δ	
	Value, % IACS	Δ, %	Value, MPa	Δ, %	Value, MPa	Δ, %	Value, %	Δ, %
Al-0.5Fe								
CAAW	57.2±0.2	2.1	170 ± 3	0.0	201 ± 1	1.5	3.7 ± 0.3	30.2
AAW [25]	58.4±0.2		170 ± 12		204 ± 14		5.3 ± 0.3	
CAAW+230 °C, 1 h	58.5±0.2	1.2	168 ± 17	4.0	207 ± 18	3.4	2.2 ± 0.4	47.8
AAW+230 °C, 1 h [25]	59.2±0.2		175 ± 11		200 ±16		4.6 ± 0.4	
Al-1.7Fe								
CAAW	51.5±0.2	0.9	150 ± 22	36.2	293 ± 1	0.7	6.6 ± 0.2	25.8
AAW [25]	52.0±0.2		235 ± 18		295 ± 19		4.9 ± 0.5	
CAAW+230 °C, 1 h	54.4±0.2	2.9	171 ± 21	31.6	260 ± 13	17.4	2.5 ± 0.2	35.9
AAW+230 °C, 1 h [25]	52.8±0.2		250 ± 14		315 ± 17		3.9 ± 0.3	

Table 2 also contains the values of the difference (in percent) in electrical conductivity and mechanical properties between the AAWs and CAAWs in the similar conditions. This information is contained in the Δ columns and is calculated as a value of the AAW subtracted from the values of the CAAW relative to the CAAW values.

In case of Al-0.5Fe alloys the difference in properties between CAAW and AAW is relatively small. Difference in σ_{YS} and σ_{UTS} lies within the error value for both CD and annealed states and could be regarded as insignificant. The Al-0.5Fe CAAW is characterized by lower electrical conductivity compared to the AAW in both states, although this difference decreases after annealing. Since electrical conductivity is sensitive to the structural defects, both on micro- and macroscale, it is natural for the aluminium wire with the core-sleeve boundary to have lower conductivity.

Al-1.7Fe CAAW is characterized by significantly lower, than in Al-1.7Fe AAW σ_{YS} in both CD and annealed states, meaning that the presence of the core-sleeve boundary contributes the faster deformation build-up [26]. In the annealed state CAAW is characterized by higher electrical conductivity and lower ductility compared to the AAW. The effect of decreased ductility in the annealed Al-1.7Fe alloys was documented in previous studies, although the exact mechanism of it is yet not clear [27,28]. One possible explanation could be the annealing-induced change of the texture formed during cold drawing, that could influence the electrical conductivity by 1 % IACS [29,30]. While Al-0.5Fe alloy demonstrates almost complete indifference (with an exception for the ductility) to the presence of the core-sleeve boundary, Al-1.7Fe demonstrates certain amount of sensitivity to the presence of such boundary.

Figure 2 presents the engineering stress-strain curves for the Al-0.5Fe alloy wires (a) and Al-1.7Fe alloy wires (b). The form and the shape of the Al-0.5Fe curves, as well as levels of the σ_{UTS} are very similar. The curves for the Al-1.7Fe are spread more, with the difference in both elongations to failure and σ_{UTS}, supporting the core-sleeve boundary having more significant influence in the Al-1.7Fe alloy rather than Al-0.5Fe. For both Al-0.5Fe and Al-1.7Fe (AAW and CAAW) alloys annealing results in the decrease of the elongation to failure. On Fig. 2(b) it could be seen that AAW to CAAW transition increases the ductility of the Al-1.7Fe alloy wire, which is contrary for the Al-0.5Fe alloy wires. Since

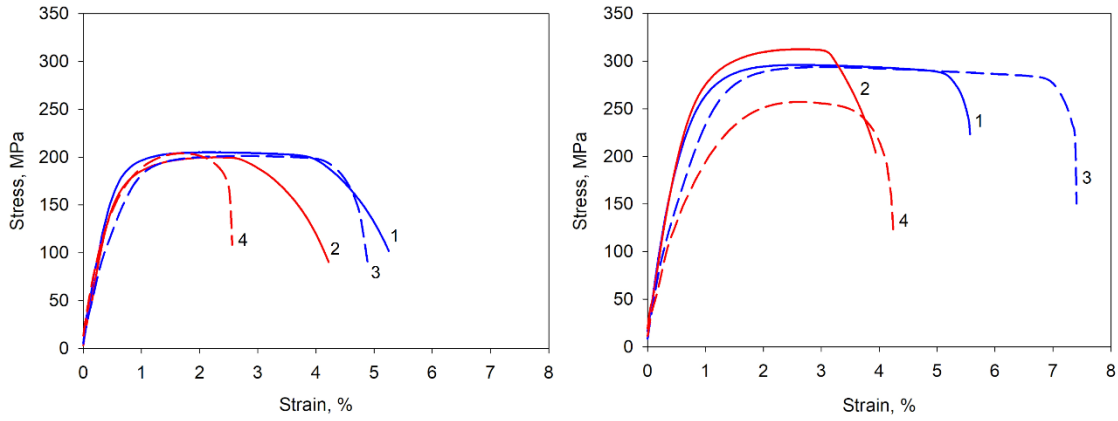

Fig. 2. Engineering stress-strain curves foe the Al-0.5Fe (a) and Al-1.7Fe (b) alloy wires: 1 – AAW in cold-drawn state; 2 - AAW after annealing at 230 °C for 1 h; 3 – CAAW in cold-drawn state; 4 - CAAW after annealing at 230 °C for 1 h

the reason for the different behavior of the AAW and CAAW may as well be attributed to the behavior of their individual components, fractography analysis was conducted.

Figure 3 demonstrates the overview of the fracture images of Al-Fe AAW (a,c) and CAAW (b,d) after tensile tests. Al-0.5Fe AAW demonstrates higher value of relative reduction, which corresponds to higher value of elongation to failure (Table 2). Similar behavior is demonstrated by the sleeve of the CAAWs (Fig. 3(b,d)).

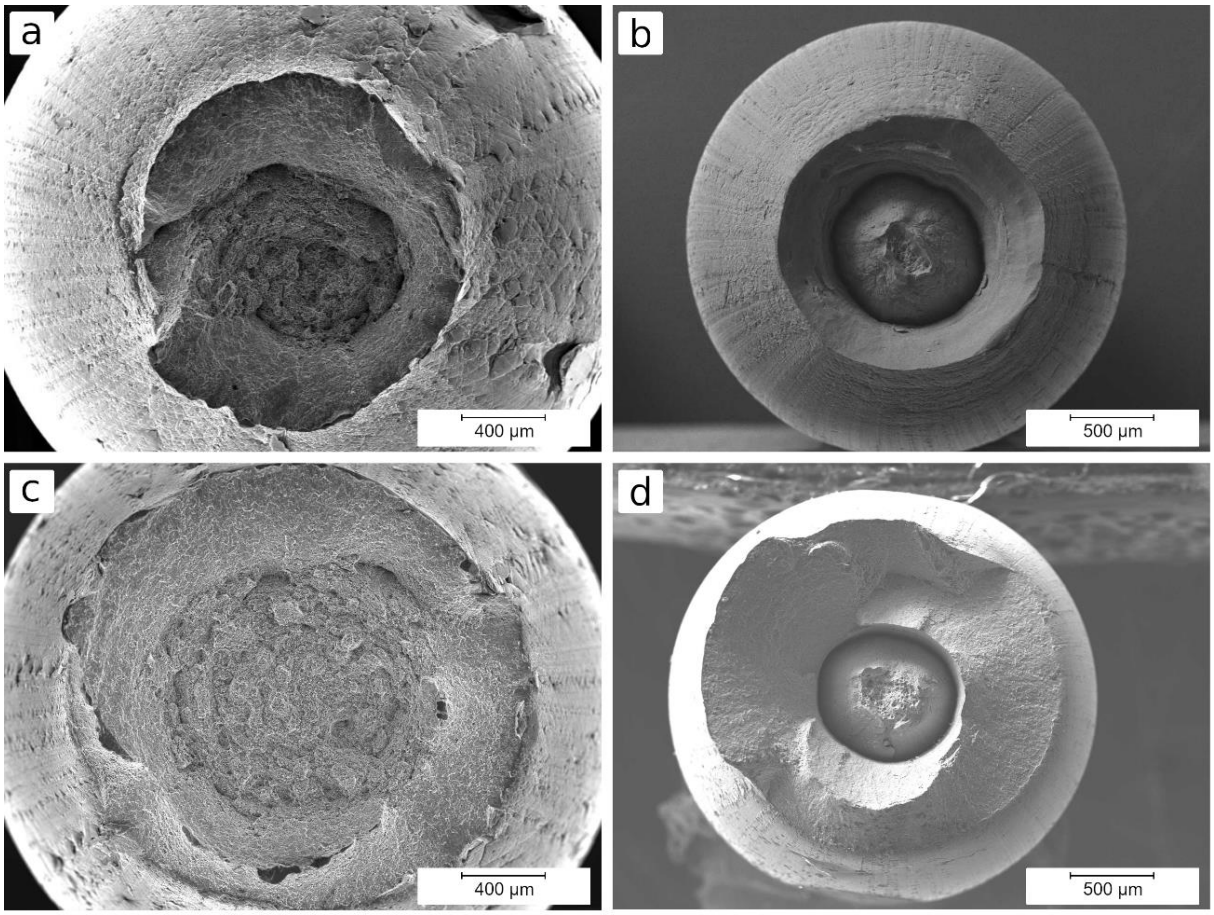

Fig. 3. Fractographic images of the (a) Al-0.5Fe AAW, (b) Al-0.5Fe CAAW, (c) Al-1.7Fe AAW and (d)Al-1.7Fe CAAW, SEM

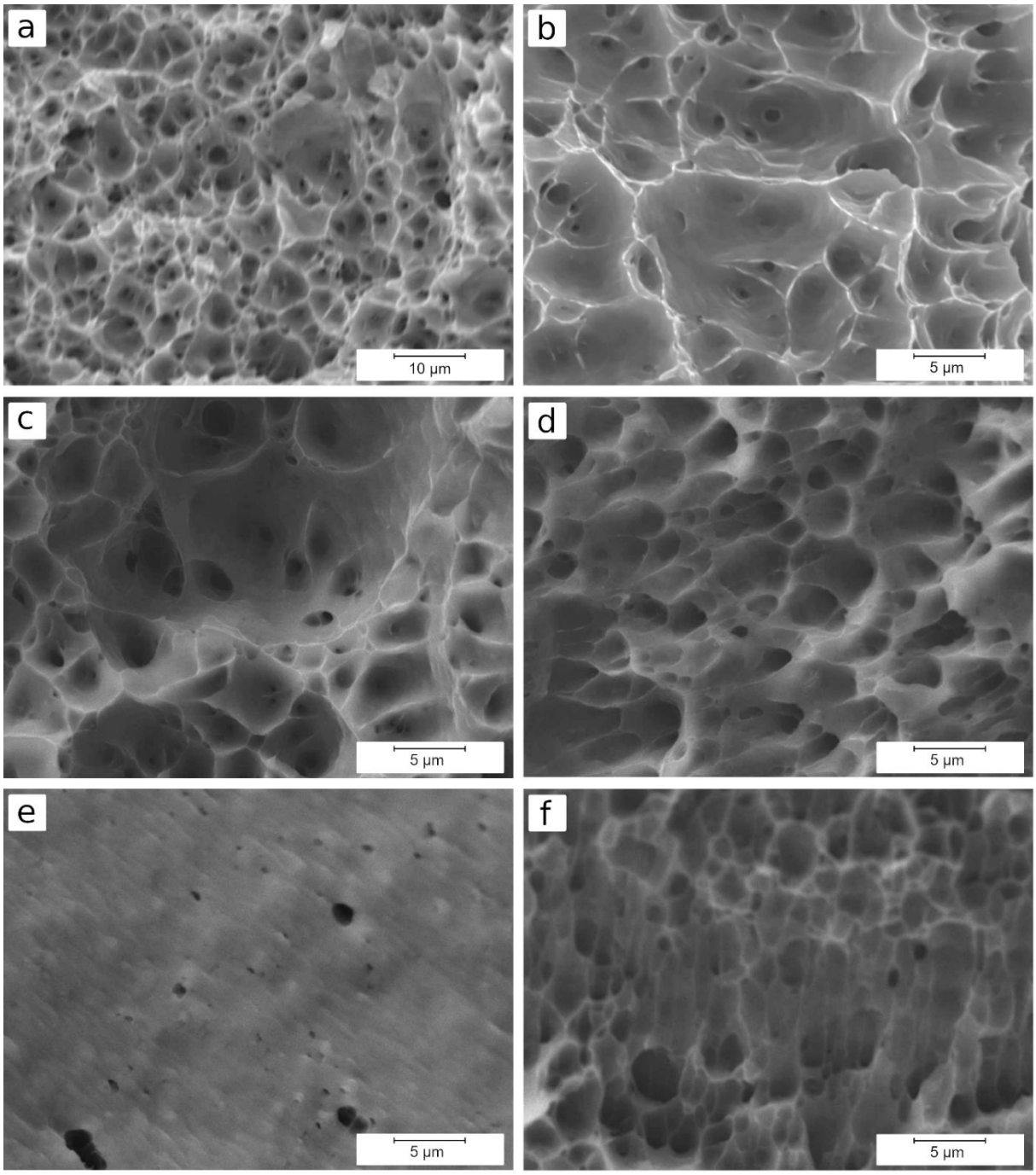

Fig. 4. Fractographic images of the Al-0.5Fe alloy wires in the initial state (a,c,e) and after annealing at 230 °C for 1 h (b, d, f), SEM: (a,b) AAW center, (c,d) CAAW core, (e,f) CAAW sleeve

Figure 4 demonstartes the fracture surface of the Al-0.5Fe wires in cold-drawn state and after annealing. The fracture of the Al-0.5Fe AAW (Fig. 4(a)), as well as fracture of the core (Fig. 4(c)) and sleeve (Fig. 4(e)) of the Al-0.5Fe CAAW are ductile in nature. Both Al-0.5Fe AAW and core of the Al-0.5Fe CAAW are characterized by the dimples, notably smaller in Al-0.5Fe AAW. The presence of the core-sleeve interfcae in the Al-0.5Fe CAAW may cause the uneven deformation within the core and sleeve of the composite wire, resulting in lowed deformation value of the core material and thus larger dimple size. The fracture surface of the Al-0.5Fe CAAW may support this hypothesis – the dimples in this region are the smallest among all three, and the fracture has smoothened surface,

probably caused by the flow of the metal during the last stage of the composite wire fraction – the core in Al-0.5Fe CAAW fractured first, the sleeve fractured later.

Annealing of the Al-0.5Fe AAW resulted in slightly lower, within the error range, ductility, with the same character of the fracture – ductile (Fig. 4(b,d,f)) for the AAW, CAAW core and CCAW sleeve, respectively). The size of the dimples is comparable to ones in the cold-drawn AAW. Annealing seem to have no effect on the core of the Al-0.5Fe CAAW, while the size and the character of the dimples in the sleeve have changed – the became larger and more pronounced. Since it was assumed that the sleeve of the CAAW accumulated higher deformation value, it is safe to asssume that the sleeve structure experienced recovery and\or recrystallization, resulting in the different dimple morphology.

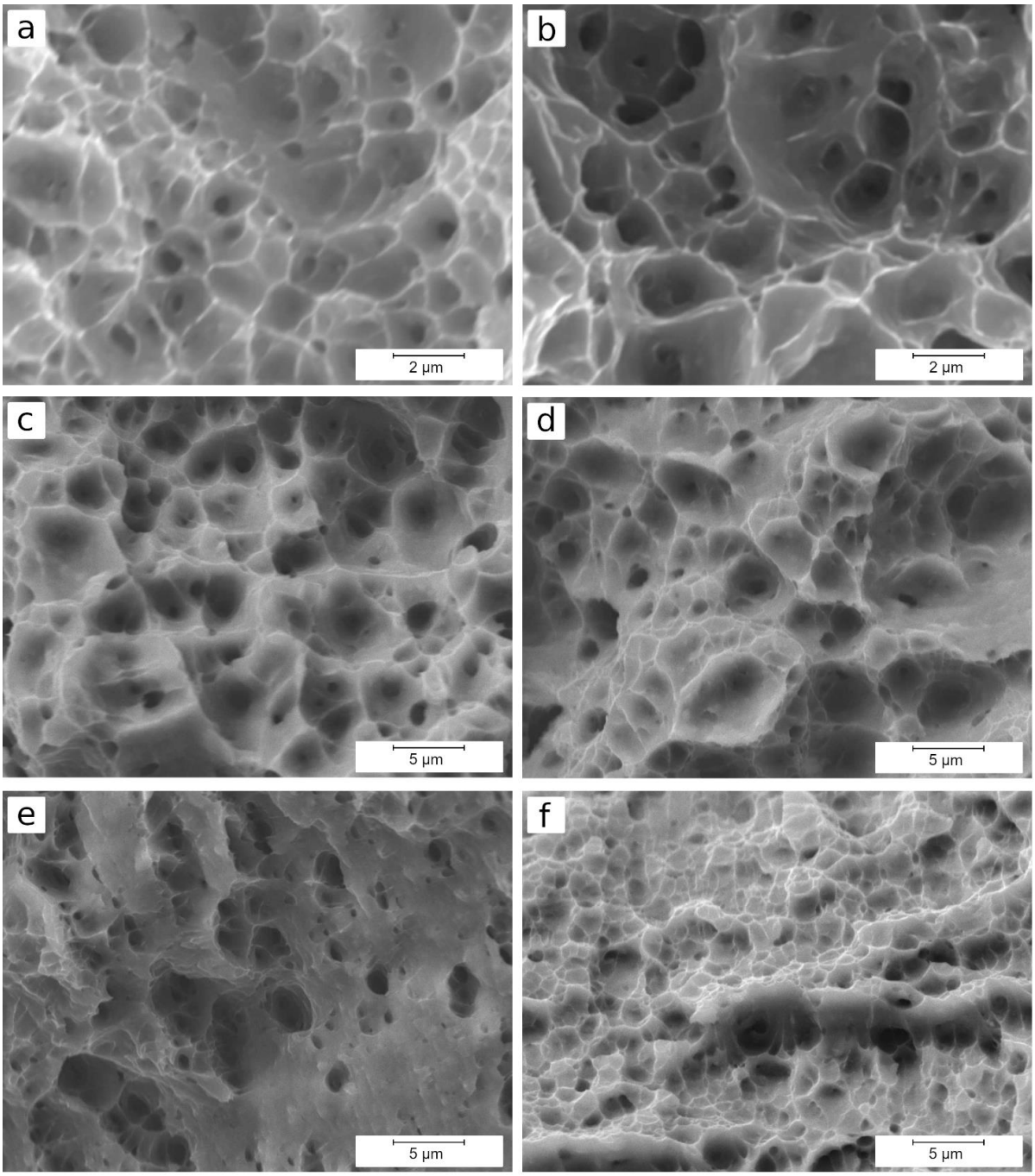

Fig. 5. Fractographic images of the Al-1.7Fe alloy wires in the initial state (a,c,e) and after annealing at 230 °C for 1 h (b,d,f), SEM: (a,b) AAW center, (c,d) CAAW core, (e,f) CAAW sleeve

Figure 5 demonstartes the fracture surface of the Al-1.7Fe wires in CD state and after annealing. The fracture of the Al-1.7Fe AAW (Fig. 4(a)), as well as fracture of the core (Fig. 4(c)) and sleeve (Fig. 4(e)) of the Al-1.7Fe CAAW are ductile in nature, similar to the Al-0.5Fe wires.

The dimple size in the Al-1.7Fe AAW is notably lower than that of Al-1.7Fe CAAW core or sleeve. It would appear that the core-sleeve boundary interface has accomodated certain amount of deformation that went directly into the material structure in AAW. Thus, less deformed core and sleeve of the Al-1.7Fe CAAW allowed higher degree of deformation before fracture and conaeequently ductilty (Fig. 2(b)).

Annealing of Al-1.7Fe wires doesn't demonstrate notable effect on the type of the AAW fracture. The dimple size remains the same. In the Al-1.7Fe CAAW influence of the annealing is similar to one in Al-0.5Fe CAAW – the form and size of simples in the core remains the same, while the sleeve demonstrates changes (in case of Al-1.7Fe CAAW - diminishing) in dimple size. This effet is most probably connected to higher accumulated deformation in the Al-1.7Fe CAAW sleeve and is manifested by increased ductility of the annealed CAAW (Fig. 2(b)).

Conclusions

In this study the core-sleeve boundary interface was introduced into the Al-0.5Fe and Al-1.7Fe alloys wires. The fraction of the core in the cross section was 10 %, and the length of the interface is 30% of the outer wire diameter. Composite all-aluminium wires (CAAW) were subjected to annealing at 230 °C for 1 h. Following conclusions were drawn:
1. In this particular case the gap width ranged from nanometer scale up to 300 nm. Presene of the core-sleeve boundary interface mildly affects the mechanical strength and electrical conductivity of the CAAW. This effect almost absent in Al-0.5Fe alloy wires, and more prominent in the Al-1.7Fe wires. Since amount of the Fe determines the intensity of the structural defects in Al-Fe alloys, the core-sleeve boundary interface impact in composite wires depends on the sensitivity of a given alloy to deformation and heat treatment.
2. It would seem that the presence of the core-sleeve boundary interface attributes to the slower build-up of the structural defects, which is supported by the lower angle of the strain-stress curve elastic region for both Al-0.5Fe and Al-1.7Fe CAAW. This could be due to the fact that core-sleeve boundary interface helps to accomodate some amount of deformation during tensile tests, that otherwise would impact the alloy itself since the pressence of this boundary affect mainly ductility and ultimate tensile strength of the CAAWs.

CRediT authorship contribution statement

Andrey E. Medvedev: writing – review & editing, writing – original draft; **Aygul F. Shaikhulova**: investigation; **Mikhail M. Motkov**: data curation; **Maxim Yu. Murashkin**: conceptualization.

Conflict of interest

The authors declare that they have no conflict of interest.

References

1. Dursun T, Soutis C. Recent developments in advanced aircraft aluminium alloys. *Mater Des*. 2014;56: 862–871.
2. Beygelzimer Y, Kulagin R, Estrin Y. Severe plastic deformation as a way to produce architectured materials. In: Estrin Y, Bréchet Y, Dunlop J, Fratzl P. (eds.) *Architectured Materials in Nature and Engineering. Springer Series in Materials Science, vol 282*. Cham: Springer; 2019, p.231–255.
3. Estrin Y, Krishnamurthy VR, Akleman E. Design of architectured materials based on topological and geometrical interlocking. *Journal of Materials Research and Technology*. 2021;15: 1165–1178.
4. Ragazin A, Aryshenskii E, Aryshenski V, Rasposienko D, Lukyanchuk A, Konovalov S. Effect of Hafnium on the Microstructure Formation during High-Temperature Treatment of High-Magnesium Aluminum Alloys Microalloyed with Scandium and Zirconium. *Phys Mesomech*. 2025;28: 535–546.
5. Soleymani S, Abdollah-Zadeh A, Alidokht SA. Microstructural and tribological properties of ultra fine grained hybrid composite produced by friction stir processing. *Materials Physics and Mechanics*. 2013;17(1): 6–10.
6. Kalombo RB, Araújo JA, Ferreira JLA, da Silva CRM, Alencar R, Capra AR. Assessment of the fatigue failure of an All Aluminium Alloy Cable (AAAC) for a 230 kV transmission line in the Center-West of Brazil. *Eng Fail Anal*. 2016;61: 77–87.
7. Zhang J, Li X, Zhao L, Li Z, Wang S, Yao P, Dai P. Analysis of Temperature Rise Characteristics and Fatigue Damage Degree of ACSR Broken Strand. *Energy Engineering*. 2023;120(3): 617–631.
8. Udensi SC, Anioke AU. An in-depth investigation of factors responsible for optimal performance in stir-cast Aluminum metal matrix composites. *Sci Afr*. 2024;26: e02452.
9. Parvizi P, Jalilian M, Dearn KD. Beyond traditional conductors: Aluminium conductor composite core's role in next-generation high temperature-low sag technologies – A review. *Electric Power Systems Research*. 2025;239: 111251.
10. Huang Y, Liu Y, Xiao Z, Huang Y. A trade-off between mechanical strength and electrical conductivity of Al–Zn–Mg–Cu alloy via Ag alloying and retrogression re-aging heat treatment. *Materials Science and Engineering: A*. 2023;880: 145230.
11. Yang C, Masquellier N, Gandiolle C, Sauvage X. Multifunctional properties of composition graded Al wires. *Scr Mater* 2020;189: 21–24.
12. Yousefi Mehr V, Toroghinejad MR. On the texture evolution of aluminum-based composites manufactured by ARB process: a review. *Journal of Materials Research and Technology*. 2022;21: 1095–1109.
13. Mei XM, Mei QS, Li JY, Li CL, Wan L, Chen F, Chen ZH, Xu T, Wang YC, Tan YY. Solid-state alloying of Al-Mg alloys by accumulative roll-bonding: Microstructure and properties. *J Mater Sci Technol*. 2022;125: 238–251.
14. Satjabut P, Uthaisangsuk V. Effects of Initial Microstructure on Mechanical Properties of AA1050/AA2024 Laminated Metal Composite Fabricated by Accumulative Roll Bonding Process. *Metals and Materials International*. 2025;31: 1460–1478.
15. Toroghinejad MR, Jamaati R, Dutkiewicz J, Szpunar JA. Investigation of nanostructured aluminum/copper composite produced by accumulative roll bonding and folding process. *Mater Des*. 2013;51: 274–279.
16. Sajjadi Nikoo S, Qods F, Yousefieh M. Microstructure evolution and mechanical properties of the AA2024/AA5083 ultra-fine grained composite fabricated via accumulative roll bonding (ARB) method. *J Mater Res*. 2023;38: 2519–2533.
17. Gashti SO, Fattah-Alhosseini A, Mazaheri Y, Keshavarz MK. Effects of grain size and dislocation density on strain hardening behavior of ultrafine grained AA1050 processed by accumulative roll bonding. *J Alloys Compd*. 2016;658: 854–861.
18. Li J, Nian Y, Liu X, Zong Y, Tang X, Zhang C, Zhang L. Application of electromagnetic metallurgy in continuous casting: A review. *Progress in Natural Science: Materials International*. 2024;34(1): 1–11.
19. International Electrotechnical Commission. IEC 62641:2023. *Conductors for overhead lines - Aluminium and aluminium alloy wires for concentric lay stranded conductors*. IEC; 2023.
20. ASTM International. ASTM E8/E8M-22. *Tension Testing of Metallic Materials*. ASTM; 2022.
21. Lee JE, Bae DH, Chung WS, Kim KH, Lee JH, Cho YR. Effects of annealing on the mechanical and interface properties of stainless steel/aluminum/copper clad-metal sheets. *J Mater Process Technol*. 2007;187–188: 546–549.
22. Saller BD, Hu T, Ma K, Kurmanaeva L, Lavernia EJ, Schoenung JM. A comparative analysis of solubility, segregation, and phase formation in atomized and cryomilled Al–Fe alloy powders. *J Mater Sci*. 2015;50: 4683–4697.
23. Saller BD, Sha G, Yang LM, Liu F, Ringer SP, Schoenung JM. Iron in solution with aluminum matrix after non-equilibrium processing: an atom probe tomography study. *Philos Mag Lett*. 2017;97(3): 118–124.

24. Medvedev AE, Zhukova OO, Khafizova ED, Motkov MM, Murashkin MYu. Composite Coaxial Wire Produced from Electromagnetically Cast Al–Fe Alloys. *Russian Journal of Non-Ferrous Metals*. 2024;65: 307–317.
25. Medvedev A, Zhukova O, Fedotova D, Murashkin M. The mechanical properties, electrical conductivity, and thermal stability of a wire made of Al–Fe alloys produced by casting into an electromagnetic crystallizer. *Frontier Materials & Technologies*. 2022;3–1: 96–105.
26. Selyutina NS. Influence of Mg and Cu on the dynamic yield stress of aluminium alloys. *Materials Physics and Mechanics*. 2021;47(3): 408–415.
27. Medvedev A, Murashkin M, Enikeev N, Medvedev E, Sauvage X. Influence of morphology of intermetallic particles on the microstructure and properties evolution in severely deformed al-fe alloys. *Metals*. 2021;11(5): 815.
28. Medvedev A, Zhukova O, Enikeev N, Kazykhanov V, Timofeev V, Murashkin M. The Effect of Casting Technique and Severe Straining on the Microstructure, Electrical Conductivity, Mechanical Properties and Thermal Stability of the Al–1.7 wt. % Fe Alloy. *Materials*. 2023;16(8): 3067.
29. Hou JP, Li R, Wang Q, Yu HY, Zhang ZJ, Chen QY, Ma H, Wu XM, Li XW, Zhang ZF. Breaking the trade-off relation of strength and electrical conductivity in pure Al wire by controlling texture and grain boundary. *J Alloys Compd*. 2018;769: 96–109.
30. Wang S, Hou JP, Zhang ZJ, Gong BS, Qu Z, Wang H, Zhou XH, Jiang HC, Wang Q, Li XW, Zhang ZF. Grain design in ultra-fine Al wire with remarkable combination of strength and conductivity: Ultra-fine-long grains with super strong 〈111〉 texture. *Scr Mater*. 2024;238: 115746.